

2016

Development of Compact and High-efficient Scroll Compressor with Novel Bearing Structure

Sungyong Ahn

Air Conditioning Compressor Team, LG Electronics Inc., sungyong.ahn@lge.com

Junchul Oh

Air Conditioning Compressor Team, LG Electronics Inc., junchul.oh@lge.com

Junghoon Park

Air Conditioning Compressor Team, LG Electronics Inc., junghoon13.park@lge.com

Seheon Choi

Air Conditioning Compressor Team, LG Electronics Inc., seheon.choi@lge.com

Byeongchul Lee

Air Conditioning Compressor Team, LG Electronics Inc., byeongchul.lee@lge.com

See next page for additional authors

Follow this and additional works at: <https://docs.lib.purdue.edu/icec>

Ahn, Sungyong; Oh, Junchul; Park, Junghoon; Choi, Seheon; Lee, Byeongchul; Cho, Hyunwoong; and Kim, Jeonghun, "Development of Compact and High-efficient Scroll Compressor with Novel Bearing Structure" (2016). *International Compressor Engineering Conference*. Paper 2483.

<https://docs.lib.purdue.edu/icec/2483>

This document has been made available through Purdue e-Pubs, a service of the Purdue University Libraries. Please contact epubs@purdue.edu for additional information.

Complete proceedings may be acquired in print and on CD-ROM directly from the Ray W. Herrick Laboratories at <https://engineering.purdue.edu/Herrick/Events/orderlit.html>

Authors

Sungyong Ahn, Junchul Oh, Junghoon Park, Seheon Choi, Byeongchul Lee, Hyunwoong Cho, and Jeonghun Kim

Development of Compact and High-efficient Scroll Compressor with Novel Bearing Structure

Sungyong AHN¹, Junchul OH^{1*}, Junghoon PARK¹, Seheon CHOI¹,
Byeongchul LEE¹, Hyunwoong CHO², Jeonghun KIM²

¹Air Conditioning Compressor Team, LG Electronics Inc.
Seoul, Korea

E-mail: sungyong.ahn@lge.com

²Air Conditioning Compressor Development Team, LG Electronics Inc.
Changwon, Gyeongnam, Korea

* Corresponding Author

ABSTRACT

High-Side Shell(HSS) scroll compressors have been widely used for Variable Refrigerant Flow(VRF) system which is a powerful solution for the cooling and heating of commercial buildings. In order to improve the characteristics of the VRF system, a new HSS scroll compressor has been developed with the outer bearing structure. The core elements of the outer bearing structure are an outer-type bush bearing mounted on an orbiting scroll and a female-type eccentric journal inside a shaft. The outer-type bush bearing which is made of engineering plastic without a back steel layer has been newly developed. The new HSS scroll compressor employing the outer bearing structure has a compact size, high efficiency, and low noise level compared to a conventional HSS scroll compressor. In order to confirm the advantages of the new HSS scroll compressor, basic tests and theoretical analysis have been performed in this study.

1. INTRODUCTION

The compression part of a scroll compressor is composed of two scrolls. One is a Fixed Scroll(F/S) which is usually clamped onto a Main Frame(M/F). The other is an Orbiting Scroll(O/S) that has orbit motion by an eccentric journal and an Oldham's couple ring. The scroll compressor has relatively a low noise and vibration level, and large capacity among positive displacement compressors because multi-chambers for compression are formed between two scrolls at the same time. Characteristics described above are the main reasons to use a scroll compressor in various heating, ventilating, and air conditioning systems. In general, the scroll compressor are classified into two types, Low-Side Shell(LSS) type and High-Side Shell(HSS) type, according to a pressure level in a compressor shell below the M/F. Variable Refrigerant Flow(VRF) systems used for cooling and heating of commercial buildings usually employ the HSS scroll compressor because that has good volumetric efficiency and the ease of oil management in addition to basic good characteristics of the scroll compressor.

Recently, the main issues of compressors for the VRF system are compact size and high efficiency. The high efficiency of VRF system is essential because regulations for building energy consumption have been reinforced with the environment issue such as global warming. Compact compressors can enhance the space utilization and cost competitiveness of the VRF system. Additionally, a heating capacity in cold weather and a noise level are basic characteristics which must meet the needs of customers using the VRF system. We have developed a new HSS scroll compressor with the outer bearing structure to raise the competitiveness of the VRF system. The core of the outer bearing structure is an outer-type bush bearing driving an O/S. The newly developed HSS Scroll compressor is represented in Fig. 1 with a conventional one, and the specifications of the two scroll compressors are listed in Table 1. The two scroll compressors have the same orbiting radius and suction volume. Furthermore, a compression

volume ratio and O/S mass are very similar comparing the two scroll compressors. That is, the two compressors are identical in terms of a capacity and theoretical motor torque required for a compression process. The main difference between the two compressors is the design of an O/S journal bearing. The O/S journal bearing of the conventional scroll compressor is designed with a male-type eccentric journal and a traditional Polytetrafluoroethylene (PTFE) bush bearing. Meanwhile, the O/S journal bearing of the new one is modeled with a female-type eccentric journal inside a shaft and an outer-type bush bearing made of engineering plastic without a steel layer. These changes in the new HSS scroll compressor bring many advantages such as compact size, high efficiency, and low noise level.

At the beginning of scroll compressor history, Inaba *et al.*[3] and Yamamora Muramatsu *et al.*[4] studied for similar type scroll compressors to the new scroll compressor. Moreover, some manufacturers produced scroll compressors which adopt the female-type eccentric journal. However, they didn't use the outer-type bush bearing. The new scroll compressor is the world's first one of which O/S journal bearing is designed with the outer-type bush bearings. In this study, basic test items of a compressor such as efficiency and a noise level are evaluated to compare the two scroll compressors each other. The lubrication characteristics of two bush bearings are also compared by bench tests. Furthermore, a theoretical analysis for shaft dynamics and the lubrication characteristics of journal bearings is performed to confirm shaft motion and journal bearing loads.

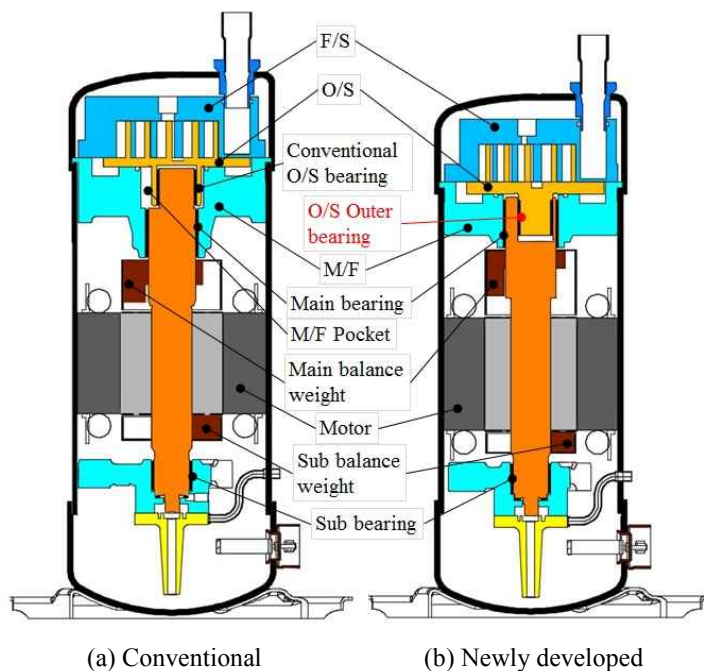


Figure 1: Comparison of scroll compressors

Table 1: Spec. of scroll compressors

Item	Conventional	Newly developed
O/S bearing type (Lubricating surface)	Inner	Outer
Weight	38kg	32kg (84%)
Height	460mm	440mm (96%)
Inner diameter	160mm	147mm (92%)
Operating speed	15~150Hz	12~165Hz

2. NEW OUTER-TYPE BUSH BEARING

While the shaft of a scroll compressor rotates synchronized with a rotor, the O/S of a scroll compressor has orbit motion. That means the loading point of a gas force is not changed in the circumferential direction of an eccentric journal as Fig. 2. The certain area of the eccentric journal sweeps all surfaces of an O/S bearing circumferentially, although the minimum clearance point on the eccentric journal is varied by shaft motion and an attitude angle. The operating mechanism of the new scroll compressor is equal to that of the conventional one. Therefore, the outer-type bush bearing should be applied to the O/S.

It is also possible to insert a bush bearing into the female-type eccentric journal in terms of manufacture. However, there are two problems in that case. One is the one-point wear of the bush bearing due to the operating mechanism of a scroll compressor mentioned above. The other is the excessive diameter of a main journal. The diameter of the main journal must be grown by twice the thickness of the bush bearing in the case. In a design using the outer-type bush bearing, the main journal already has slightly larger diameter than that of the conventional scroll compressor to

secure shaft stiffness of the minimum thickness point by the female-type eccentric journal. The diameter of the main journal has to be minimized in an available design range to reduce bearing loss. Therefore, the outer-type bush bearing made of engineering plastic is mounted on the O/S like as Fig. 3(b). The traditional PTFE bush can't be used as the outer-type bearing because that has a slit.

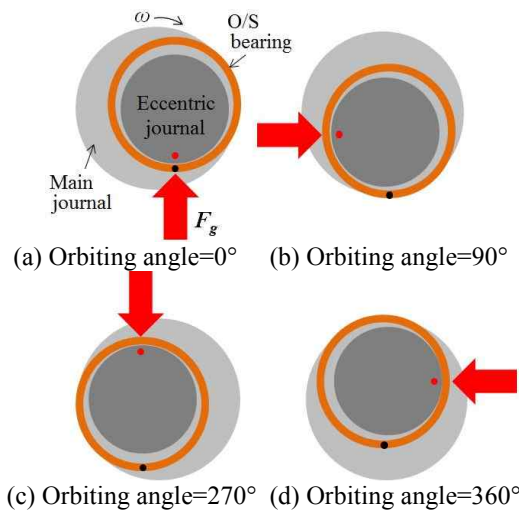


Figure 2: Acting direction of gas force

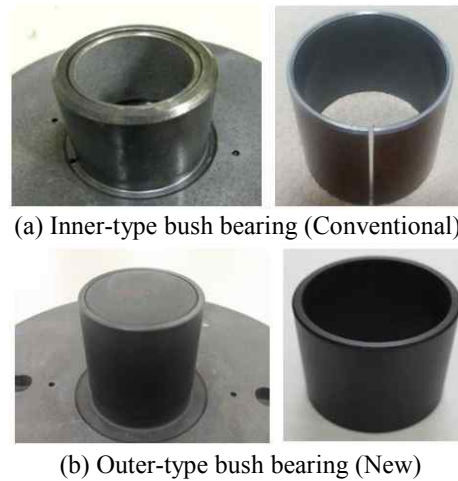


Figure 3: Bush bearings for O/S journal bearing

All development processes of the outer-type bush bearing are focused on its reliability for high temperature oil and refrigerant in a compressor. Additives and thermal treatment processes have a key role in the reliability. Figure 4 shows the test results of bush bearings using a bench tester for the journal bearing of a scroll compressor. The new bush bearing made of an engineering plastic is compared with two kinds of bush bearings to confirm its feasibility. One is the PTFE bush bearing used for the conventional scroll compressor. The other is an Aluminum(Al) bush bearing which is well known for its low friction coefficient in a hydrodynamic lubrication region. Figure 4(a) represents the Stribeck curves of the three bush bearings from a step load test (60Hz, $\mu=0.005\text{Pa}\cdot\text{s}$). The curve of the new bush bearing is located between two curves of the PTFE bush and Al bush bearing. That means the new bush bearing has a medium characteristics between the PTFE and Al bush bearing in terms of friction loss. The oil block test results are presented in Fig. 4(b). Oil supply is suddenly blocked during a normal operation (60Hz, 3000N, $\mu=0.005\text{Pa}\cdot\text{s}$). While the Al bush bearing has short duration time after oil block, the new bush bearing and PTFE bush bearing has quite larger duration time than the Al bush. From the results, it is confirmed that the new bush bearing has typical good characteristics of two existing bearings.

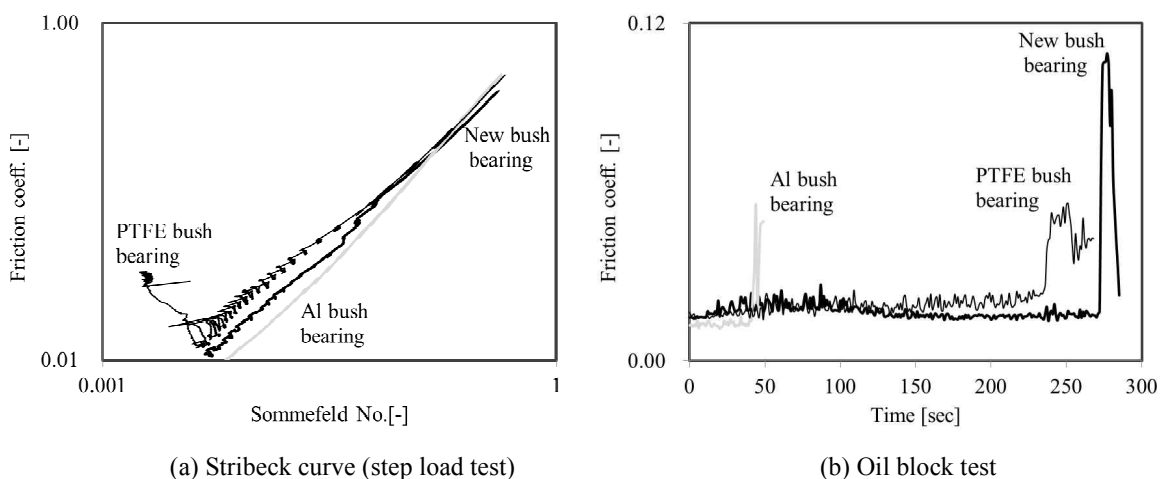


Figure 4: Results of bearing tests

The Sommerfeld No. in Fig. 4 (a) is a non-dimensional bearing load. That is defined as follows:

$$\text{Sommerfeld No.} = \frac{2\mu NRL}{F} \left(\frac{R}{c}\right)^2 \tag{1}$$

Where, μ is oil viscosity, N is the revolutions of a journal per second, R is a bearing radius, L is a bearing length, F is a bearing load, and c is a radial clearance.

3. ADVANTAGES AND TECHNOLOGIES

The main advantages of the new HSS scroll compressor are introduced in this section. The two scroll compressors illustrated in Fig. 1 are compared to each other.

3.1 Reduced journal bearing loads

As mentioned in a chapter 1, the two sources of journal bearing loads are almost identical in the two scroll compressors. One is a gas force which is the driving force of an O/S. The other is a centrifugal force by O/S orbit motion. However, main and sub journal bearing loads by the two forces are clearly different in the two scroll compressors. The simple theories of statics are used to evaluate the journal bearing loads. In this analysis, we assume that all resultant forces act on the mid-point of bearing length, and a F/S wrap completely supports the O/S centrifugal force equally over wrap height.

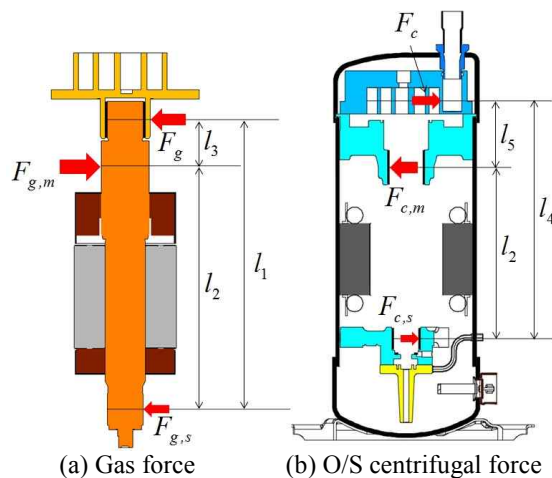


Figure 5: Journal bearing loads by gas force and O/S centrifugal force (F_g, F_c are perpendicular)

Figure 5 shows journal bearing loads by the gas force and the O/S centrifugal force. Journal bearing loads due to the gas force can be estimated by force and moment balances of a shaft as follows:

$$F_{g,m} = \frac{l_1}{l_2} F_g, F_{g,s} = F_{g,m} - F_g \tag{2}$$

Where, $F_{g,m}$ is a main journal bearing load and $F_{g,s}$ is a sub journal bearing load by the gas force. The definition of each length which represents distance between the mid points of bearing length is illustrated in Fig. 5 (a). The good designed balancing system for a compressor also should be met the force and moment balances of the stationary part of a compressor. Therefore, journal bearing loads by the O/S centrifugal force can be expressed as follows:

$$F_{c,m} = \frac{l_4}{l_2} F_c, F_{c,s} = F_{c,m} - F_c \tag{3}$$

Table 2: Journal bearing loads by gas force

Item	Load (normalized by O/S bearing load)	
	Conventional	New
O/S (Gas force)	1.00	
Main	1.18	1.02 (86%)
Sub	0.18	0.02 (11%)

Table 3: Journal bearing loads by O/S centrifugal force

Item	Load (normalized by O/S centrifugal force)	
	Conventional	New
O/S centrifugal force	1.00	
Main	1.39	1.23 (88%)
Sub	0.39	0.23 (59%)

Where, $F_{c,m}$ is a main journal bearing load and $F_{c,s}$ is a sub journal bearing load by the O/S centrifugal force.

From Eqns. (2) and (3), the length l_3 and l_5 in Fig. 5 have a key role in journal bearing loads due to the gas force and the O/S centrifugal force. The two lengths are reduced by the outer bearing structure in the new scroll compressor. Tables (2) and (3) list calculation results of the journal bearing loads using Eqns. (2) and (3). All journal bearing loads of the new scroll compressor are reduced compare to the conventional scroll compressor. That has very important meaning because the reduced journal bearing loads should be helpful for all characteristics of the new scroll compressor.

3.2 Compact design

In a chapter 3.1, the O/S centrifugal force is reviewed with the force and moment balances of the stationary part without balance weights. Considering the equilibrium of the moving part, the balance weights of the new scroll compressor have a smaller unbalanced mass than the balance weights of the conventional one. There are two main reasons. One is a female-type eccentric journal. It can offset some unbalanced mass of an O/S, while the mass of a male-type eccentric journal is added to the unbalanced mass of the O/S. The other is reduced distance between the mass center of the O/S and that of a main balance weight, which is similar to the principle of reduced journal bearing loads in Eqn. (2). The reduced unbalanced mass of balance weights has a key role in the compactness of a scroll compressor when the outer radius of a balance weight has to be decreased.

Some technologies including the outer bearing structure are adopted to the new scroll compressor to implement its compactness. Those are listed in Table 4 compared to the conventional scroll compressor.

Table 4: Technologies for compact scroll compressor

Part	Item	Specification (%) (Normalized by conventional value)		Technology
		Conventional	New	
O/S	Plate diameter	100%	94%	Hybrid wrap design
F/S	Thrust area	100%	80%	Optimization of back pressure mechanism (Outer bearing structure)
Shaft	Length	100%	92%	Outer bearing structure
Main balance weight	Unbalanced	100%	71%	Outer bearing structure
Sub balance weight	mass	100%	63%	Outer bearing structure
Motor	Volume	100%	94%	High power motor design

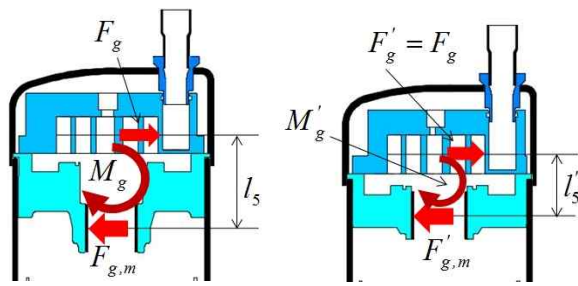
In Table 4, The outer bearing structure has a key role in the optimization of back pressure mechanism because a back pressure seal size can be reduced. While the back pressure seal size of the conventional scroll compressor is constrained by a M/F pocket size, that of the new scroll compressor is constrained by a main bearing size. The available minimum seal diameter of the new scroll compressor is 89% of that of the conventional one. The M/F pocket is denoted in Fig. 2.

3.3 Low noise

The noise level of the new scroll compressor is lower than the conventional scroll compressor in all operating conditions. In particular, the noise level is reduced by 4.0dB(sound power level) at 150Hz heating condition. Although both the reduced journal bearing loads and the compact size of the new scroll compressor have good effects on the noise, we think those are not main effects of the improvement. we compare the noise level of the new scroll compressor with another conventional type scroll compressor. The capacity of that is two-third of the new scroll compressor, and the size of that is equal to the new scroll compressor. The noise level of the new scroll compressor is slightly lower than the another conventional type scroll compressor. That means the new scroll compressor has a certain effect which compensate for the increase of compressor capacity in terms of noise.

The main reason for noise reduction would be lower exciting moments produced by the gas force and the O/S centrifugal force. Figure 6 represents the exciting moments produced by the gas force in the two scroll compressors. The gas force, F_g , acts on the F/S and O/S journal bearing simultaneously, and the main journal bearing should support a load by the gas force, $F_{g,m}$. These two forces cause a huge moment because the F/S and M/F is combined as one body. Furthermore, the moment excites compressors. If a M/F and compressor shell are combined by welding points, the moment would be a reason for fatigue fracture of the welding points. In Fig. 6 (a), l_5 can be considered by a moment arm which is coupled with F_g and $F_{g,m}$. The ratio l'_5 in Fig. 5 (b) to l_5 is 0.62, and $F'_{g,m}$ to $F_{g,m}$ is 0.86.

Consequently, The ratio of the compressor exciting moment due to the gas force, M'_g to M_g , is estimated at 0.57. A compressor exciting moment by the O/S centrifugal force also reduced by the same principle as described earlier. This effect has been a main reason for the development of the new scroll compressor because it is essential to reduce compressor noise in high speed operations.



(a) Conventional (b) New

Figure 6: Exciting moment due to O/S centrifugal force

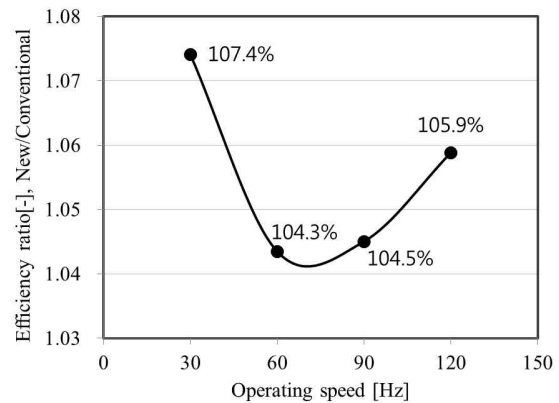


Figure 7: Compressor efficiency at rated condition (Evaporating temp.=7.2°C, Condensing temp.=54.4°C)

3.4 Efficiency improvement

Figure 7 shows the efficiency improvement of the new scroll compressor at a rated condition. The efficiency of the new scroll compressor is improved more than 5% compared to the conventional one. Especially, the efficiency improvement is remarkable at low speed and high speed conditions.

Even if we can list all items of the efficiency improvement, it is very difficult to quantify each item because of interactions between the items. However, some roles of the outer bearing structure for the efficiency improvement can be explained qualitatively. The reduced bearing loads which is explained in a chapter 3.1 clearly helpful in efficiency improvement in all operating conditions, and the outer-type bush bearing has a lower friction coefficient than the traditional PTFE bush bearing. The stirring loss in the M/F pocket which is usually filled with an oil is also eliminated by the outer bearing structure. Finally, the outer bearing structure helps the optimization of a thrust bearing as reducing back pressure seal size.

4. ANALYSIS OF SHAFT DYNAMICS AND BEARINGS

Shaft dynamics and journal bearings are analyzed to confirm the eccentricities and loads of journal bearings. In this analysis, it is assumed that F/S wrap completely support the O/S centrifugal force, and O/S tilting motion is synchronized with a shaft. Therefore, the O/S journal bearing is analyzed with the most favorable condition, while main and sub journal bearings should support all centrifugal forces. Figure 8 shows forces and coordinate systems applied to this analysis. Centrifugal forces by the unbalanced mass of shaft, main balance weight, and sub balanced weight are considered in this analysis. The weight of shaft assembly is also considered to confirm its z direction motion. The gas force which is equally applied to the two compressors in this analysis is represented in Fig. 9. The gas force is calculated by theoretical analysis with the rated operating condition denoted in Fig. 7. The definition of orbiting angle is represented in Fig. 2.

In order to determine the pressure distribution of journal bearings, the Reynolds equation is solved in θ -z coordinate systems:

$$\frac{1}{R^2} \frac{\partial}{\partial \theta} \left(h^3 \frac{\partial p}{\partial \theta} \right) + \frac{\partial}{\partial z} \left(h^3 \frac{\partial p}{\partial z} \right) = 6\mu\omega \frac{\partial h}{\partial \theta} + 12\mu \frac{\partial h}{\partial t} \quad (4)$$

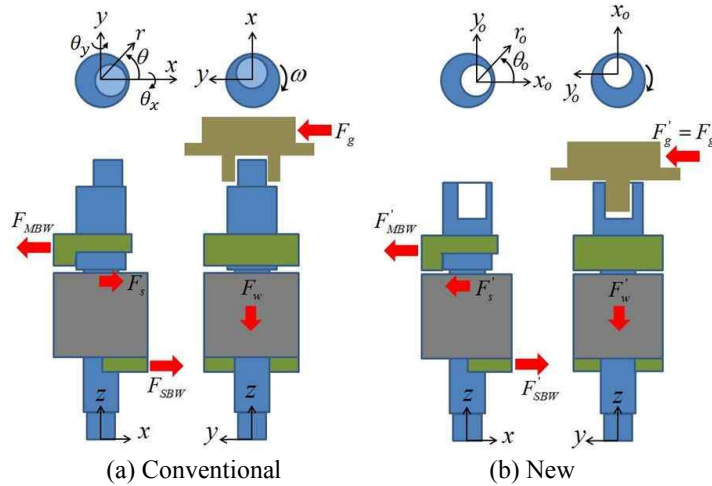


Figure 8: Forces and coordinate systems

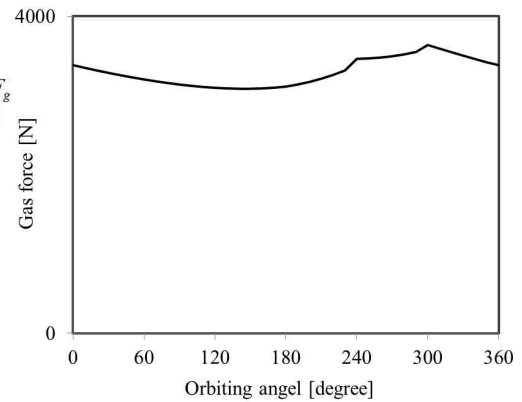


Figure 9: Gas force variations at rated condition

Where, h is clearance, p is pressure, t is time, and ω is the angular velocity of a shaft. The clearacne distribution of main and sub journal bearings can be expressed as follows:

$$h = c - u_x \cos \theta - u_y \sin \theta + z(\alpha \sin \theta - \beta \cos \theta) \tag{5}$$

Where, u_x and u_y denote shaft translation motion in x and y directions, and α and β represent shaft tilting motion in θ_x and θ_y directions respectively. The clearance distribution of an O/S journal bearing is given by:

$$\begin{aligned} \text{Conventional : } h &= c - a_x \cos \theta_o - a_y \sin \theta_o \\ \text{New : } h &= c + a_x \cos \theta_o + a_y \sin \theta_o \end{aligned} \tag{6}$$

A new coordinate system of which origin is the O/S journal center is needed for the O/S journal bearing analysis. The new coordinate system have orbit motion synchronized with a shaft rotation. θ_o in Eqn. (6) denotes the circumferential direction of the new coordinate system. a_x and a_y represent O/S translation motion in x_o and y_o directions in the new coordinate system respectively. The subscript o means the new coordinate system. The Reynolds equation for the O/S journal bearing is not represented because its form is the same as Eqn. (4).

Thrust bearing to support the weight of shaft assembly is also analyzed to consider z direction motion of a shaft. The Reynolds equation and clearance distribution of the thrust bearing can be expressed as follows:

$$\begin{aligned} \frac{1}{r^2} \frac{\partial}{\partial \theta} \left(h^3 \frac{\partial p}{\partial \theta} \right) + \frac{1}{r} \frac{\partial}{\partial r} \left(r h^3 \frac{\partial p}{\partial r} \right) &= 6\mu\omega \frac{\partial h}{\partial \theta} + 12\mu \frac{\partial h}{\partial t} \\ h &= u_z + r(\alpha \sin \theta - \beta \cos \theta) \end{aligned} \tag{7}$$

Where, u_z is the translation motion of the shaft in z direction.

Dynamic equations for the five-degrees-of-freedom motion of a shaft are given by:

$$\begin{aligned} m\ddot{x} &= \sum F_x = \sum F_{x,action} + \sum F_{x,reaction} & I_{xx}\ddot{\theta}_x &= \sum M_{\theta_x} = \sum M_{\theta_x,action} + \sum M_{\theta_x,reaction} \\ m\ddot{y} &= \sum F_y = \sum F_{y,action} + \sum F_{y,reaction} & I_{yy}\ddot{\theta}_y &= \sum M_{\theta_y} = \sum M_{\theta_y,action} + \sum M_{\theta_y,reaction} \\ m\ddot{z} &= \sum F_z = \sum F_{z,action} + \sum F_{z,reaction} \end{aligned} \tag{8}$$

Where, m is the mass of shaft assembly. I_{xx} and I_{yy} are the moment of inertia of shaft assembly. Subscript *reaction* represents the oil film pressure of bearings.

The Reynolds equations are solved by the finite difference method, and dynamic equations in Eqn. (8) are calculated by the Euler explicit method. Total calculation is over when the relatively error of shaft motion between the previous cycle and present cycle is below 0.5% for all orbiting angles. One orbiting cycle (orbiting angle from 0° to 360°) is divided into 20,000 steps. Oil viscosity is set to 0.005Pa·s, and c/R is fixed as 0.0015 for all journal bearings in this analysis.

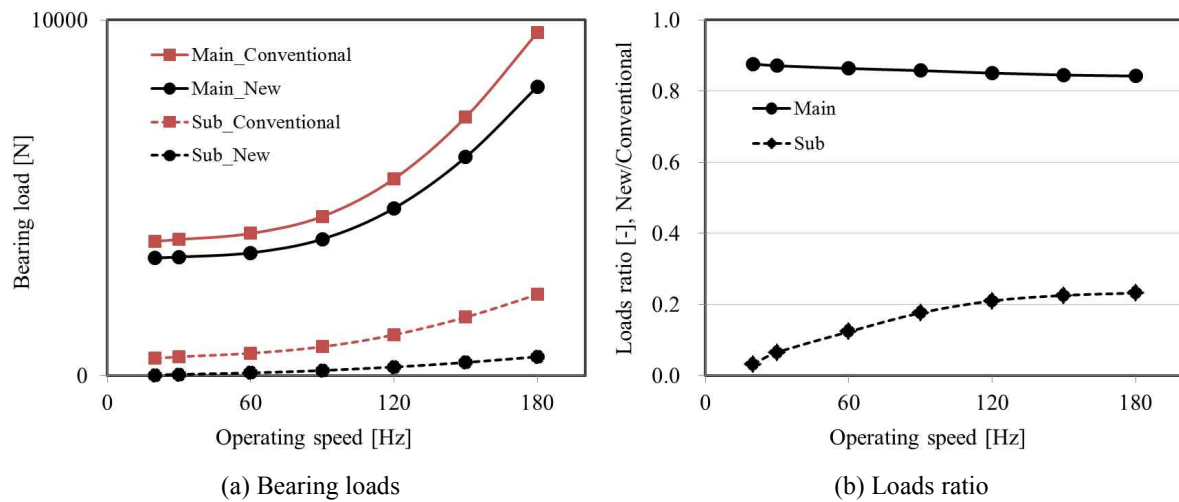


Figure 10: Comparison journal bearing loads

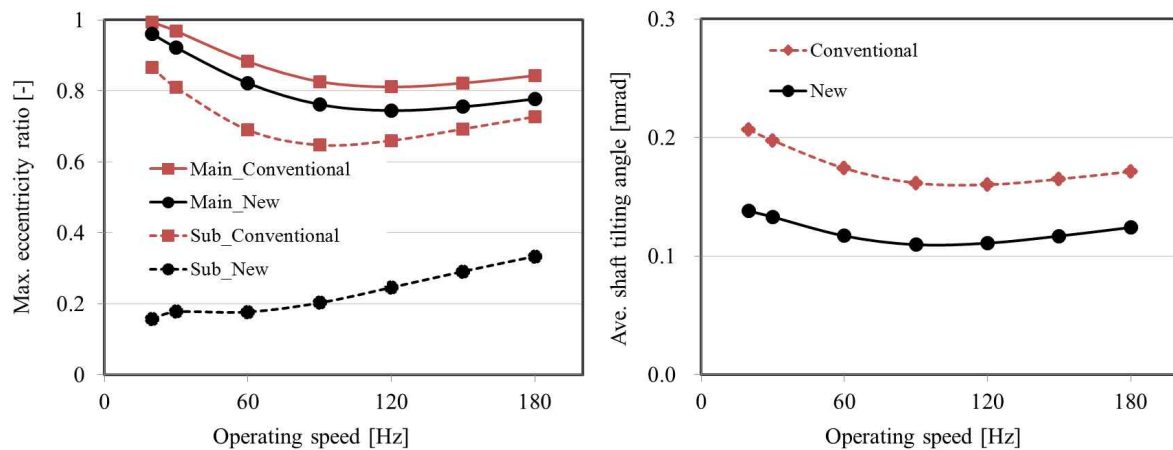


Figure 11: Max. eccentricity ratio

Figure 12: Ave. shaft tilting angle

Analysis results for the bearing loads are denoted in Fig. 10. Both main bearing load and sub bearing load of new socrll compressor are lower than the conventional one especially sub bearing load of the new one is dramatically decreased. In Fig 10 (b), the loads ratio of main bearings is about 0.87 at 20Hz. That is correspond to the result in Table 2. The gas force is dominant in the low speed conditions. The loads ratio of main bearings at 180Hz is 0.84 in Fig 10 (b). That is quite different with the result in Table 3. This difference may be caused by the assumption for a supporting point of the centrifugal force in a chapter 3.1.

Figure 11 shows the maximum eccentricity ratio of journal bearings during one rotation of a shaft. The definition of the maximum eccentricity ratio is given by:

$$\varepsilon_{max} = 1 - (h_{min} / c) \quad (9)$$

The sub journal bearing of the new scroll compressor does not significantly deviate from a concentric point in Fig. 11, and the main journal bearing of the new one also has relatively larger minimum clearance compared to the conventional one. Consequently, shaft tilting angle of the new scroll compressor is quite reduced in comparison with the conventional one as Fig.12. The reduced shaft tilting angle is good effect on the side contacts of journal bearings. The shaft tilting angle is defined as follows:

$$\text{Shaft tilting angle} = \sqrt{\alpha^2 + \beta^2} \quad (10)$$

Although the results of this analysis don't explain all advantages of the outer bearing structure which are came up in a chapter 3, the validity of the outer bearing structure for efficiency and wide operating speed is confirmed.

5. CONCLUSION

The new HSS scroll compressor with the outer bearing structure has developed for the VRF system. Compactness, high efficiency, and a low noise level are implemented by various technologies in the new scroll compressor. The outer bearing structure has a key role in the improvements.

- 1) The size of the new scroll compressor is about 80% of the conventional one. The outer bearing structure reduces shaft length and balance weight size.
- 2) The efficiency of the new scroll compressor improves more than 5% compared to the conventional one. Reduced journal bearing loads due to the outer bearing structure improve compressor efficiency in all operating conditions.
- 3) The outer bearing structure decreases the noise level by reducing the compressor exiting moment caused by the O/S centrifugal force and the gas force.
- 4) The maximum operating speed of the new scroll compressor is expanded by 165Hz. The reduced journal bearing load and low noise level have a key role in the expansion of operating speed.

NOMENCLATURE

Roman

a	Linear displacement of orbiting scroll [m]
c	Radial clearance of journal bearing [m]
F	Force [N]
F'	Force in the scroll compressor [N]
h	Clearance of bearing [m]
L	Bearing length [m]
l	Distance [m]
l'	Distance in new scroll compressor [N]
M	Moment [N m]
M'	Moment in new scroll compressor [N]
m	Mass [kg]
N	Revolution speed [rev s ⁻¹]
p	Pressure [Pa]
R	Bearing radius [m]
u	Linear displacement of shaft [m]
I_{xx}	Moment of inertia in θ_x direction [kg m ²]
I_{yy}	Moment of inertia in θ_y direction [kg m ²]

Greek

α	Angular displacement in θ_x direction [rad]
β	Angular displacement in θ_y direction [rad]
ε	Eccentricity ratio of journal bearing [-]
μ	Viscosity [Pa s]
ω	Angular velocity [rad s ⁻¹]

Sub script

1	Between sub bearing to O/S bearing
2	Between sub bearing to main bearing
3	Between main bearing to O/S bearing
4	Between sub bearing to F/S wrap
5	Between main bearing to F/S wrap
c	Centrifugal
g	Gas
m	Main bearing
s	Sub bearing

REFERENCES

- [1] C. Kim, S. Choi, Y. Cho et al., 2010, Development of High-Side Shell Scroll Compressor with Novel Oil Return Mechanism, *International Compressor Engineering Conference at Purdue*, C-15, No. 1412
- [2] B. Yoo, S. Choi, I. Won et al., 2012, Development of New High-Side Shell Scroll Compressor with Real-Time Oil Level Sensor, *International Compressor Engineering Conference at Purdue*, No. 1418
- [3] T. Inaba, M. Sugihara, T. Nakamura, T. Kimura, E. Morishita, 1986, A Scroll Compressor with Sealing Means and Low Pressure Side Shell, *International Compressor Engineering Conference at Purdue*, No. 577
- [4] M. Yamamora Muramatsu, Y. Kojima, S. Yamamoto, S. Kawahara, N. Ishii, 1990, Compact Type Scroll Compressor for Air Conditioners, *International Compressor Engineering Conference at Purdue*, No. 699